Supplementary Information

Supplementary Text S1: Modified dynamics in the 2D dynamical model

The equations (2)-(1) in the main text can be regarded as a way of calculating $\frac{\partial u}{\partial t}$ and $\frac{\partial T}{\partial t}$ given all other variables. (This is required in any calculation of the evolution of u and T.) Note that (3) and (4) can be differentiated with respect to t and combined to give a linear relation between $\frac{\partial u}{\partial t}$ and $\frac{\partial T}{\partial t}$ and (5) can be used to write each of v and w in terms of a streamfunction ψ. Then we have three coupled equations, represented symbolically as:

$$\frac{\partial u}{\partial t} + A_u\,\psi = G[u] \qquad (8)$$

$$\frac{\partial T}{\partial t} + A_T\,\psi = Q_{volc} + Q_{rad}[T] \qquad (9)$$

$$\varepsilon_u \frac{\partial u}{\partial t} + \varepsilon_T \frac{\partial T}{\partial t} = 0 \qquad (10)$$

These equations are not linear because the operators and some of the quantities on the right depend on u and on T. But at any instant $\frac{\partial u}{\partial t}$, $\frac{\partial T}{\partial t}$ and ψ are linear functions of the terms on the right-hand side, including Q_{volc} and G. Consider $A_u\,\psi$, which represents the terms including v and w in (2). Divide these into two parts ${A_u}^{(l)}\psi$ representing the Coriolis force $-2\Omega\, sin\varphi\, v$ and ${A_u}^{(nl)}\psi$ representing the advection of relative momentum by the residual mean circulation. ${A_u}^{(l)}\psi$ is the term that is responsible for the asymmetry between easterly and westerly shear zones in the QBO. ${A_u}^{(l)}\psi$ is the term that is included in all linear descriptions of the residual circulation and which allows, for example, the response to an applied heating to be distributed between a response in temperature and a response in velocity.

Now separate the above equations into two parts:

$$\frac{\partial u^{(1)}}{\partial t} + {A_u}^{(1)}\,\psi^{(1)} = G[u] \qquad (11)$$

$$\frac{\partial T^{(1)}}{\partial t} + A\,T\,\psi^{(1)} = Q_{rad}[T^{(1)}] \qquad (12)$$

$$\varepsilon_u \frac{\partial u^{(1)}}{\partial t} - \varepsilon_T \frac{\partial T^{(1)}}{\partial t} = 0 \qquad (13)$$

$$\frac{\partial u}{\partial t} + {A_u}^{(2)}\,\psi^{(2)} = 0 \qquad (14)$$

$$\frac{\partial T^{(2)}}{\partial t} + A\,T\,\psi^{(2)} = Q_{volc} + Q_{rad}[T^{(2)}] \qquad (15)$$

$$\varepsilon_u \frac{\partial u^{(2)}}{\partial t} - \varepsilon_T \frac{\partial T^{(2)}}{\partial t} = 0 \qquad (16)$$

The $u^{(1)}$, $u^{(2)}$, $T^{(1)}$ and $T^{(2)}$ fields are followed in time, with the relation $u = u^{(1)} + u^{(2)}$and $T = T^{(1)} + T^{(2)}$ being applied at all times (in particular to define the *A* operators).

If ${A_u}^{(1)} = {A_u}^{(2)} = A_u$, then the separation will have no effect. The evolution of u and T will be exactly as it was according to the original unseparated equation. (It has been verified that the numerical implementation satisfies this property.)

If ${A_u}^{(1)} = {A_u}^{(2)} = {A_u}^{(l)}$, then the effect of the separation will be the same as solving the original equations with $A_u = {A_u}^{(l)}$, i.e., the dynamics will be linear in the sense that no advection of relative momentum is taken into account. (The result will be that there is no asymmetry of QBO shear zones.)

If ${A_u}^{(1)} = A_u$ and ${A_u}^{(2)} = {A_u}^{(l)}$, then advection of relative momentum by the part of the meridional circulation induced directly by the aerosol heating will be neglected, but advection of relative momentum by the remaining part of the meridional circulation will be included. This defines the modified dynamics. The results of applying the modified dynamics to the QBO perturbation simulations are shown Figure 8. See main text for discussion.

Supplementary Text S2: Results from eruptions in January

Figure S1 shows the QBO zonal mean winds for eruptions in January (cf. Fig. 3 in the main text). We identify the same trends as outlined for July eruptions; the e-QBO is more disrupted than the w-QBO in response to a tropical eruption. In response to an eruption in January, we find a 60 Tg eruption causes the QBO phases to ascend after an eruption initiated in both a w-QBO and an e-QBO state, but 15 Tg eruptions do not cause observable ascent. Even so, the westerly phase is substantially delayed in the lower stratosphere after a 15 Tg eruption initiated during an e-QBO such that the easterly phase above descends 12 months later than in the control simulation (comparable to the delay of the 15 Tg case in July). Minor differences between the responses to an eruption in January compared to July are expected since the initial conditions including the QBO are not identical, but we conclude that the season of eruption does not noticeably impact the progression of the QBO.

Figure S2 shows the latitudinal position of the QBO westerly phase after eruptions in January (cf. Fig. 5, Sect. 3.1.3). The westerly phase of the QBO after a 60 Tg eruption initiated during a w-QBO state deviated substantially from the control simulations until 15 months after the eruption. The most notable change relative to the control is an excursion to 12° S after 5 months. The changes to the westerly phase, a general broadening and strengthening of the westerly phase in the Southern Hemisphere, can also be identified in Fig. S3c and Fig S4c. Importantly, these changes occur in the opposite hemisphere to eruption in July, but are otherwise similar in magnitude. After a 15 Tg eruption initiated during a w-QBO state in January, there are no significant changes.

Both 15 Tg and 60 Tg eruptions initiated during an e-QBO state show movement into the Southern Hemisphere compared to the control simulations, reaching 6° S and 9° S, respectively. The volcanic sulfate aerosol distribution in Fig. S3b initially shows a slightly higher distribution of sulfate in the Northern Hemisphere although after 5 months (Fig. S4b) this is no longer obvious, and in both cases the eruption during a w-QBO state shows a more asymmetrical distribution. The latitudinal movement following the e-QBO state is larger than shown for the July eruptions, possibly because the westerly phase is stronger and extends to higher altitudes at the start of the simulation for the case chosen in January. This may make the January case more sensitive to movement as the westerly phase is initially located above the temperature anomaly. Further ensemble members with a variety of e-QBO states would be needed to confirm this.

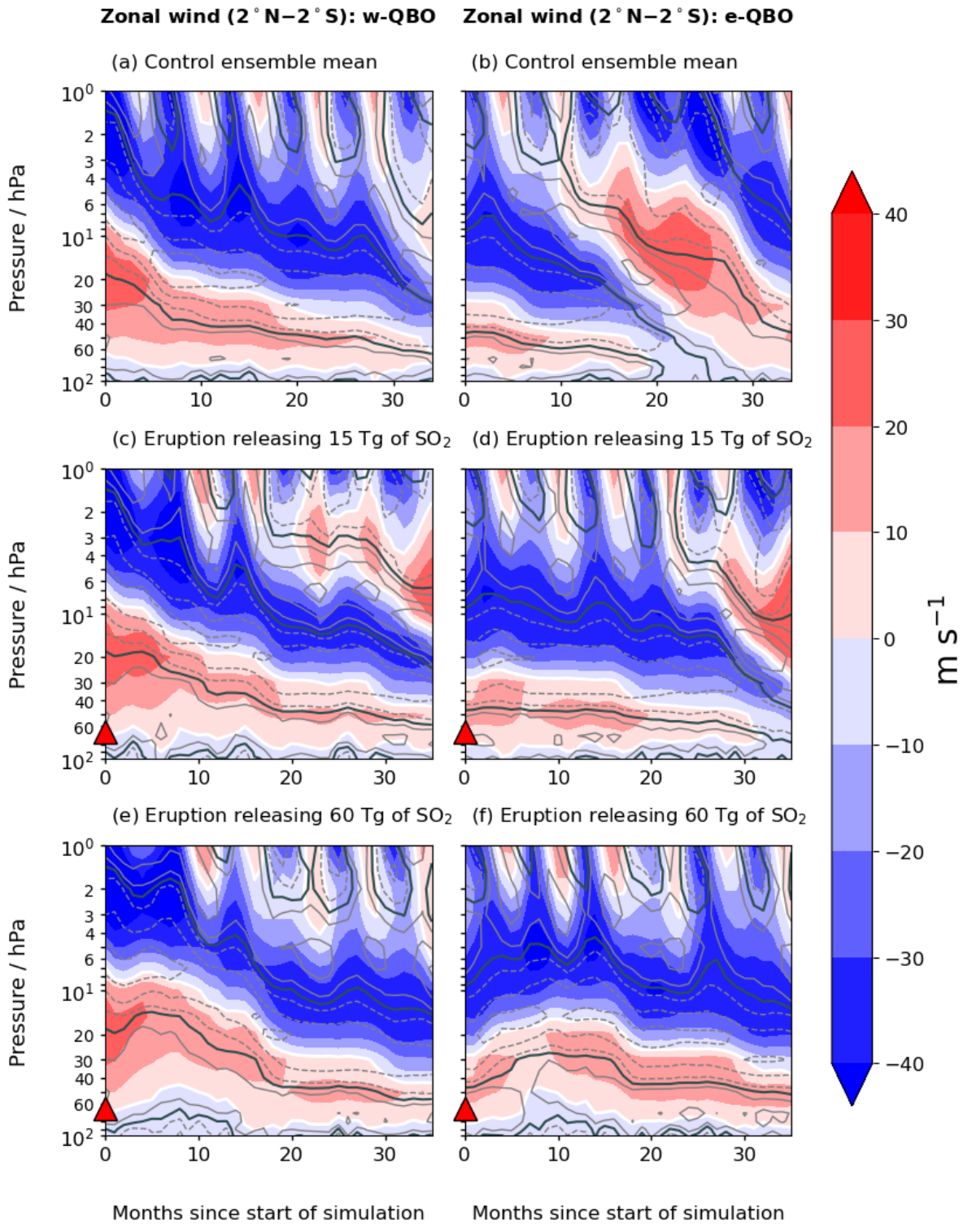

Figure S1: Filled contours: Mean zonal wind averaged 2° N – 2° S. Contour lines: Positive (solid) and negative (dashed) mean zonal wind shear (the change in wind speed with height) at intervals of 0.0025 s^{-1} averaged 2° N – 2° S. A black solid contour indicates a wind shear of zero. The left column shows simulations initiated during westerly shear at 30 hPa, and the right column shows simulations initiated during easterly shear at 30 hPa for (a), (b) the control ensemble mean (3 members), (c), (d) 15 Tg eruptions, (d), (e) 60 Tg eruptions. A white solid contour indicates the zero-wind line for comparison to Fig. 4. Red triangles indicate the approximate altitude of SO_2 injection.

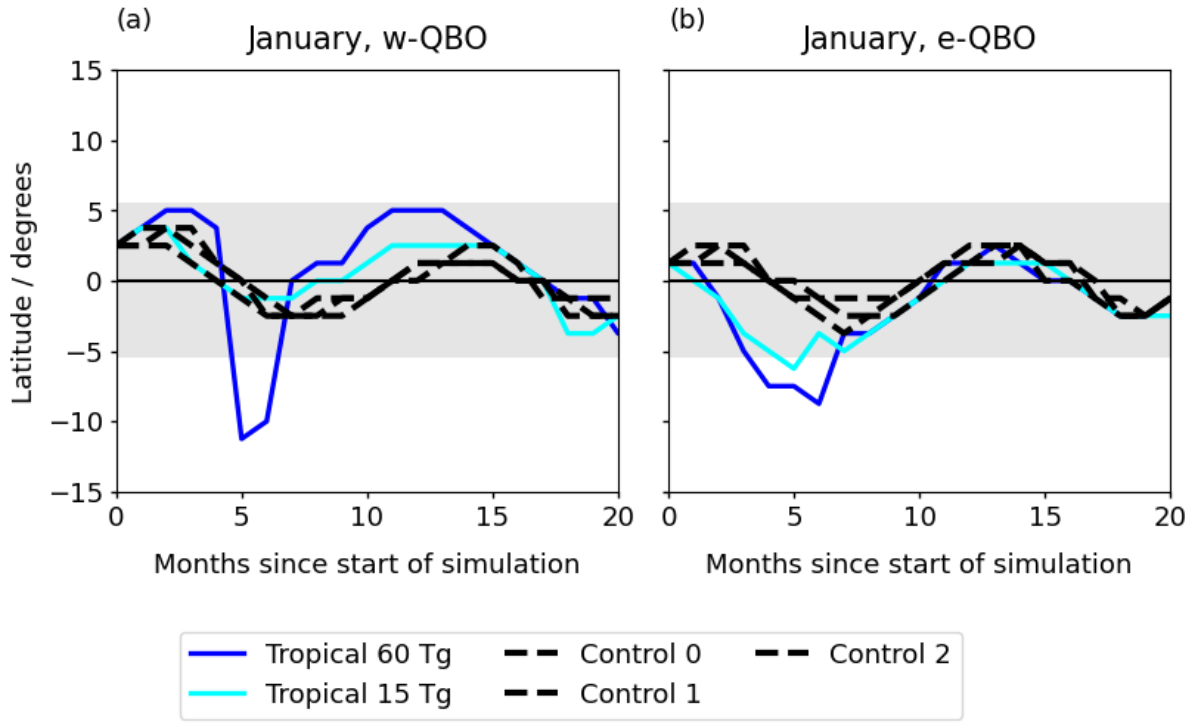

Figure S2: Latitudinal structure of the QBO for (a) eruptions initiated during a w-QBO and (b) eruptions initiated during an e-QBO. Solid lines indicate latitudinal position of the QBO westerly wind maximum in the region 10 hPa – 70 hPa, 15° N – 15° S following 60 Tg and 15 Tg eruptions and black dashed lines indicate the latitudinal position of the QBO westerly wind maximum for each of the three control ensemble members. Grey shading covers the latitudes that contain 95% of the variation in the position of the observed QBO westerly maximum.

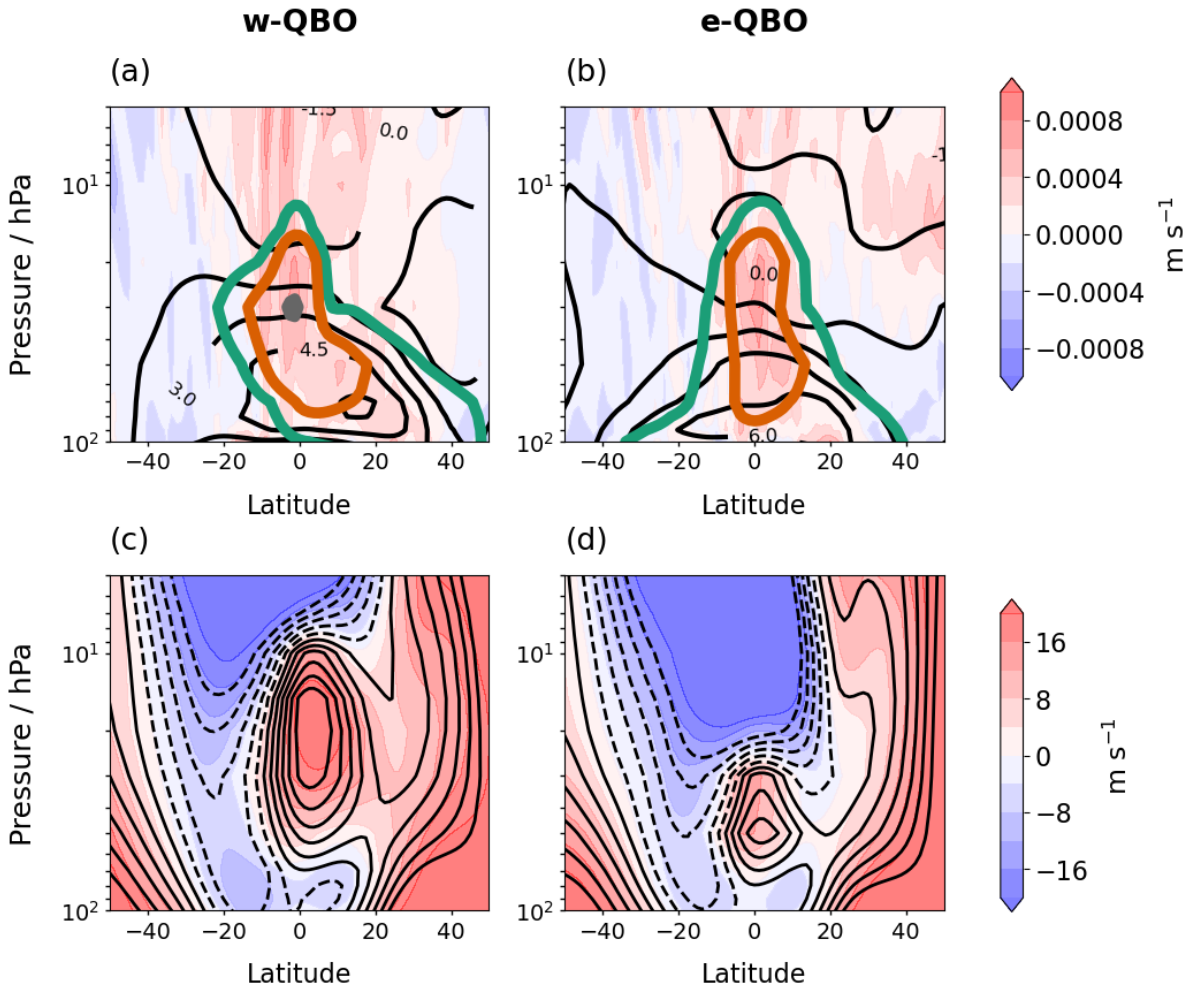

Fig. S3: Two months after 60 Tg eruptions in January: (a), (b) shows the *w* anomalies (filled contours), positive temperature anomalies (black line contours) and sulfate mass mixing ratio anomalies (coloured line contours) with respect to the control ensemble mean. The sulfate mass mixing ratio contours are at interval of 5 x10^{-8}, 15 x10^{-8}, 50 x10^{-8} kg kg^{-1} and the temperature contours are in intervals of 1.5 K. (c), (d) The monthly mean zonal wind after the eruption (filled contours) compared to the control (black line contours). The filled contour intervals are the same as the line contours, with dashed lines representing negative zonal winds in the line contours. Panels (a) and (c) show results for the w-QBO, and panels (b) and (d), for the e-QBO.

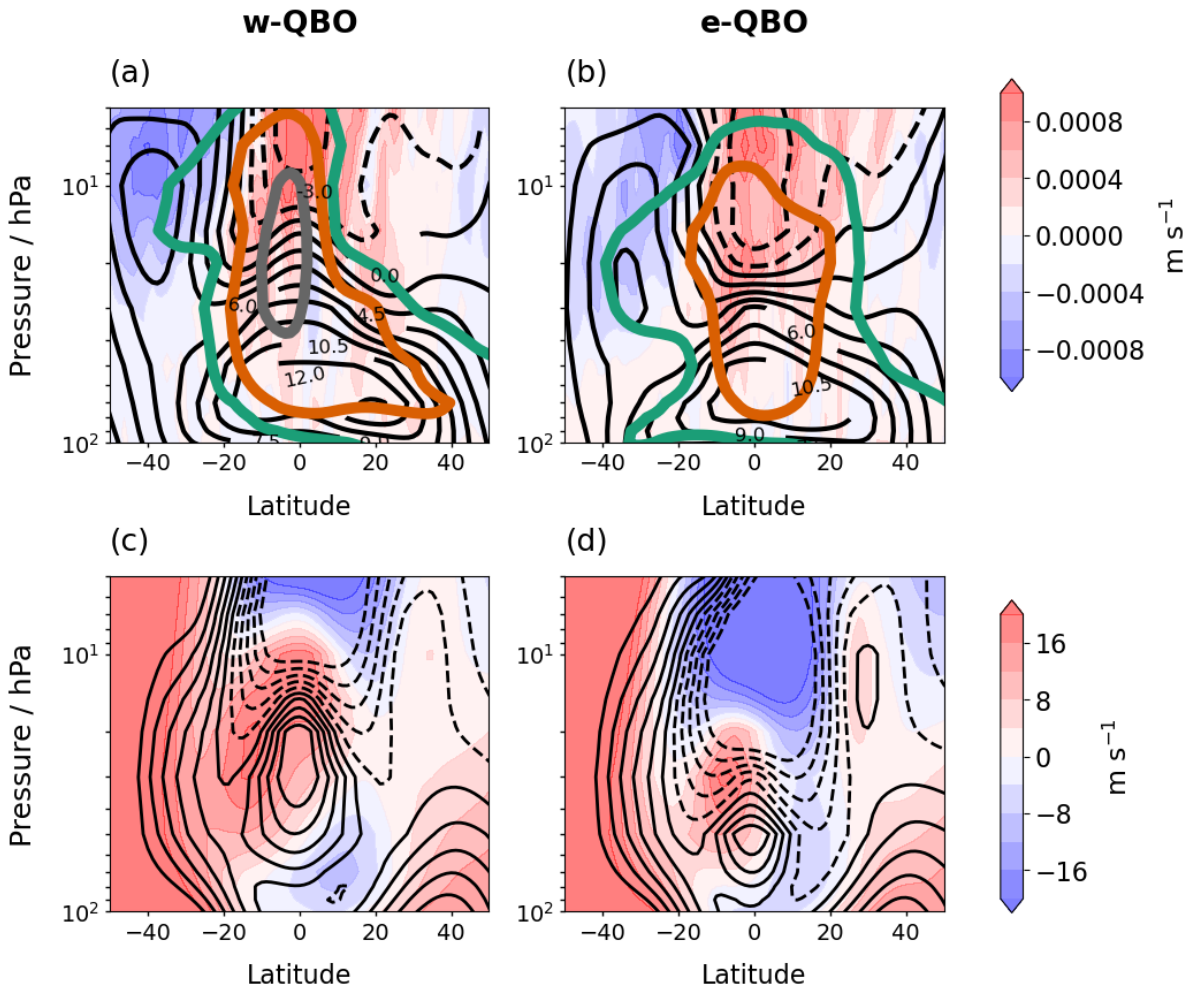

Figure S4: Five months after 60 Tg eruptions in January: (a), (b) shows the *w* anomalies (filled contours), positive temperature anomalies (black line contours) and sulfate mass mixing ratio anomalies (coloured line contours) with respect to the control ensemble mean. The sulfate mass mixing ratio contours are at interval of 5 x10^{-8}, 15 x10^{-8}, 50 x10^{-8} kg kg^{-1} and the temperature contours are in intervals of 1.5 K. (c), (d) The monthly mean zonal wind after the eruption (filled contours) compared to the control (black line contours). The filled contour intervals are the same as the line contours, with dashed lines representing negative zonal winds in the line contours. Panels (a) and (c) show results for the w-QBO, and panels (b) and (d), for the e-QBO.

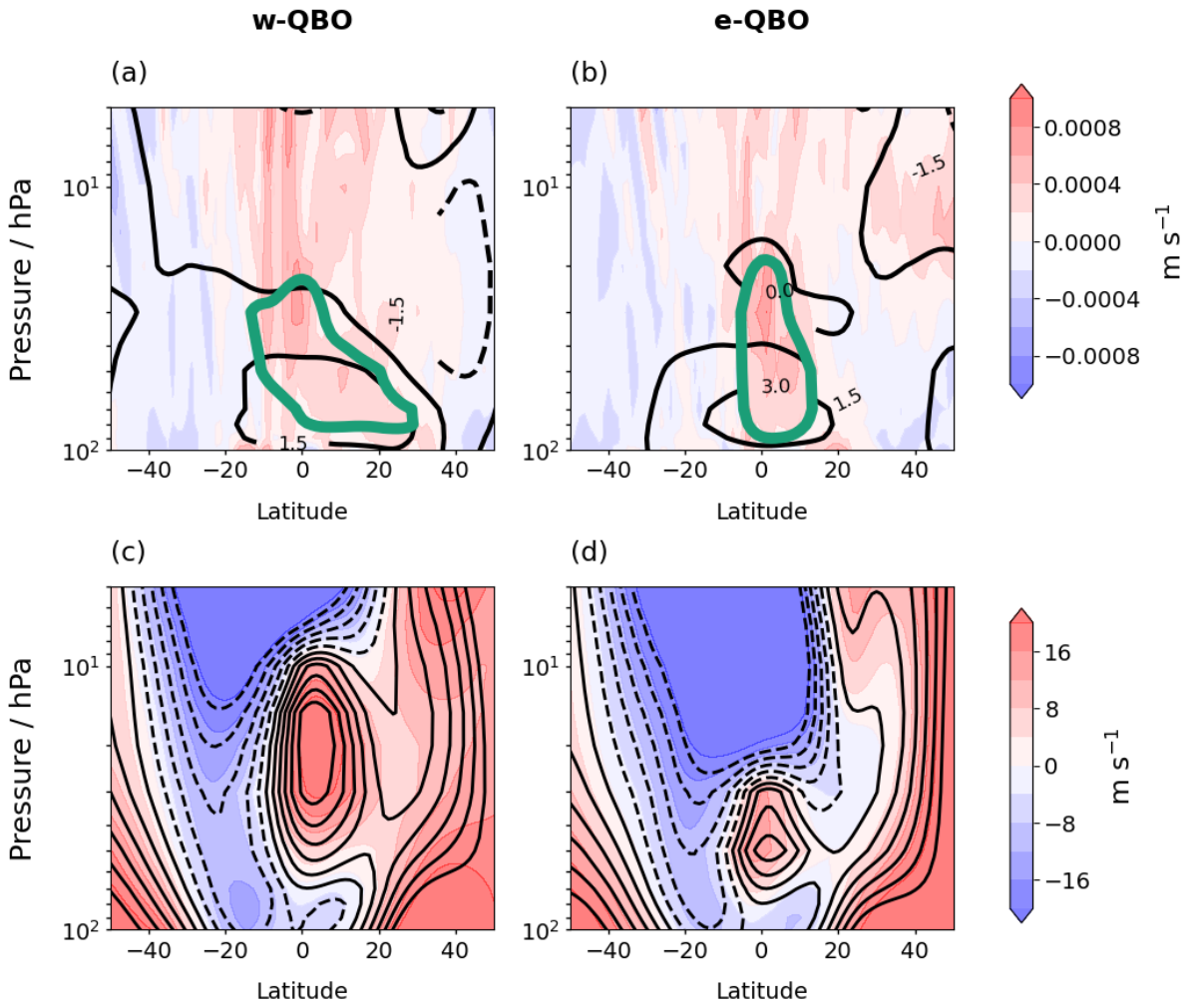

Figure S5: Two months after 15 Tg eruptions in January: (a), (b) shows the *w* anomalies (filled contours), positive temperature anomalies (black line contours) and sulfate mass mixing ratio anomalies (coloured line contours) with respect to the control ensemble mean. The sulfate mass mixing ratio contours are at interval of 5 x10^{-8}, 15 x10^{-8}, 50 x10^{-8} kg kg^{-1} and the temperature contours are in intervals of 1.5 K. (c), (d) The monthly mean zonal wind after the eruption (filled contours) compared to the control (black line contours). The filled contour intervals are the same as the line contours, with dashed lines representing negative zonal winds in the line contours. Panels (a) and (c) show results for the w-QBO, and panels (b) and (d), for the e-QBO.

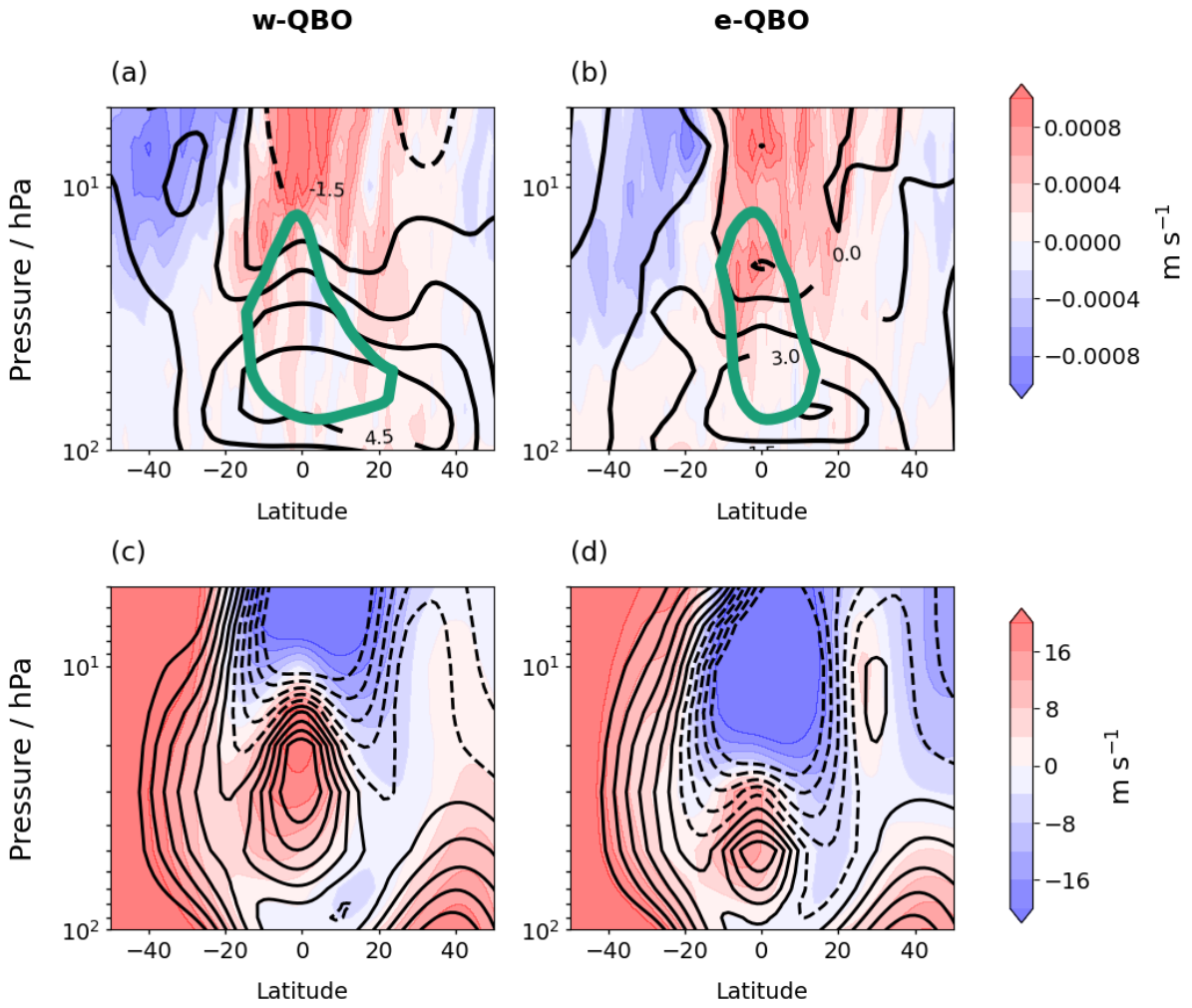

Figure S6: Five months after 15 Tg eruptions in January: (a), (b) shows the *w* anomalies (filled contours), positive temperature anomalies (black line contours) and sulfate mass mixing ratio anomalies (coloured line contours) with respect to the control ensemble mean. The sulfate mass mixing ratio contours are at interval of 5 x10^{-8}, 15 x10^{-8}, 50 x10^{-8} kg kg^{-1} and the temperature contours are in intervals of 1.5 K. (c), (d) The monthly mean zonal wind after the eruption (filled contours) compared to the control (black line contours). The filled contour intervals are the same as the line contours, with dashed lines representing negative zonal winds in the line contours. Panels (a) and (c) show results for the w-QBO, and panels (b) and (d), for the e-QBO.

Supplementary Text 3: Results for 15 Tg eruptions in July

As for the 60 Tg eruptions (Fig. 9 of the main text), initial transport of sulfate after a 15 Tg injection is strongest into the Southern Hemisphere following the w-QBO case, but for the e-QBO case the sulfate distribution is more symmetrical (Fig. S7). After five months the aerosol has begun to decay and the month with the highest burden has already passed, due to the smaller SO_2 injection and thus smaller volcanic aerosol burden compared to a 60 Tg eruption (Fig. S8). The bulk of the volcanic sulfate aerosol is still located in the Southern Hemisphere although there is increased transport into the Northern Hemisphere (Fig. S8a). The westerly phase of the QBO is strengthened in the Northern Hemisphere although the shift is smaller than for a 60 Tg eruption (cf. Fig. S8c and Fig. 10c) due to the smaller magnitude of eruption. For an eruption initiated during an e-QBO, the sulfate distribution is symmetrical and the largest change to the QBO is the increase in altitude of the phases.

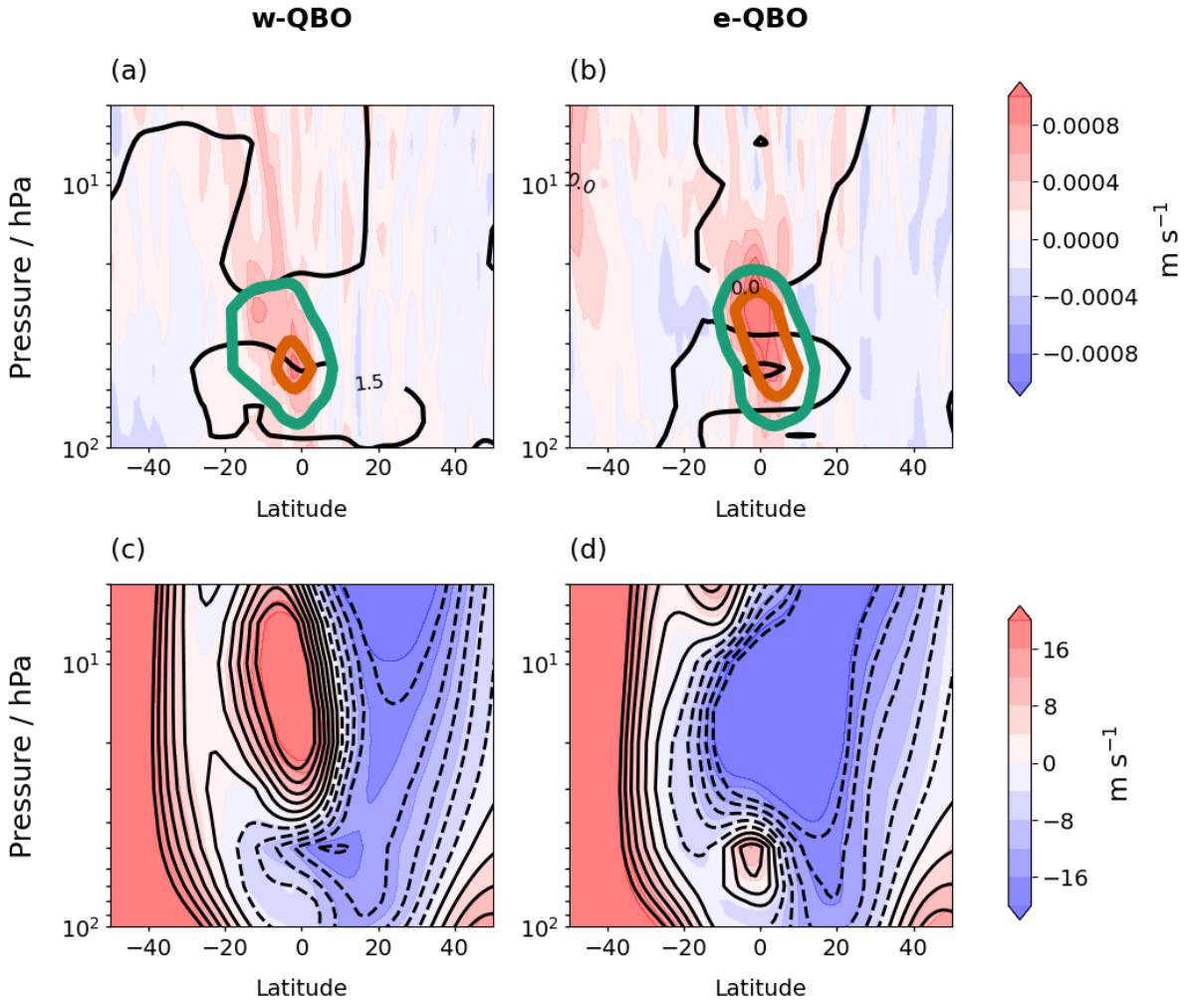

Figure S7: Two months after 15 Tg eruptions in July: (a), (b) shows the *w* anomalies (filled contours), positive temperature anomalies (black line contours) and sulfate mass mixing ratio anomalies (coloured line contours) with respect to the control ensemble mean. The sulfate mass mixing ratio contours are at interval of 5 x10^{-8}, 15 x10^{-8}, 50 x10^{-8} kg kg^{-1} and the temperature contours are in intervals of 1.5 K. (c), (d) The monthly mean zonal wind after the eruption (filled contours) compared to the control (black line contours). The filled contour intervals are the same as the line contours, with dashed lines representing negative zonal winds in the line contours. Panels (a) and (c) show results for the w-QBO, and panels (b) and (d), for the e-QBO.

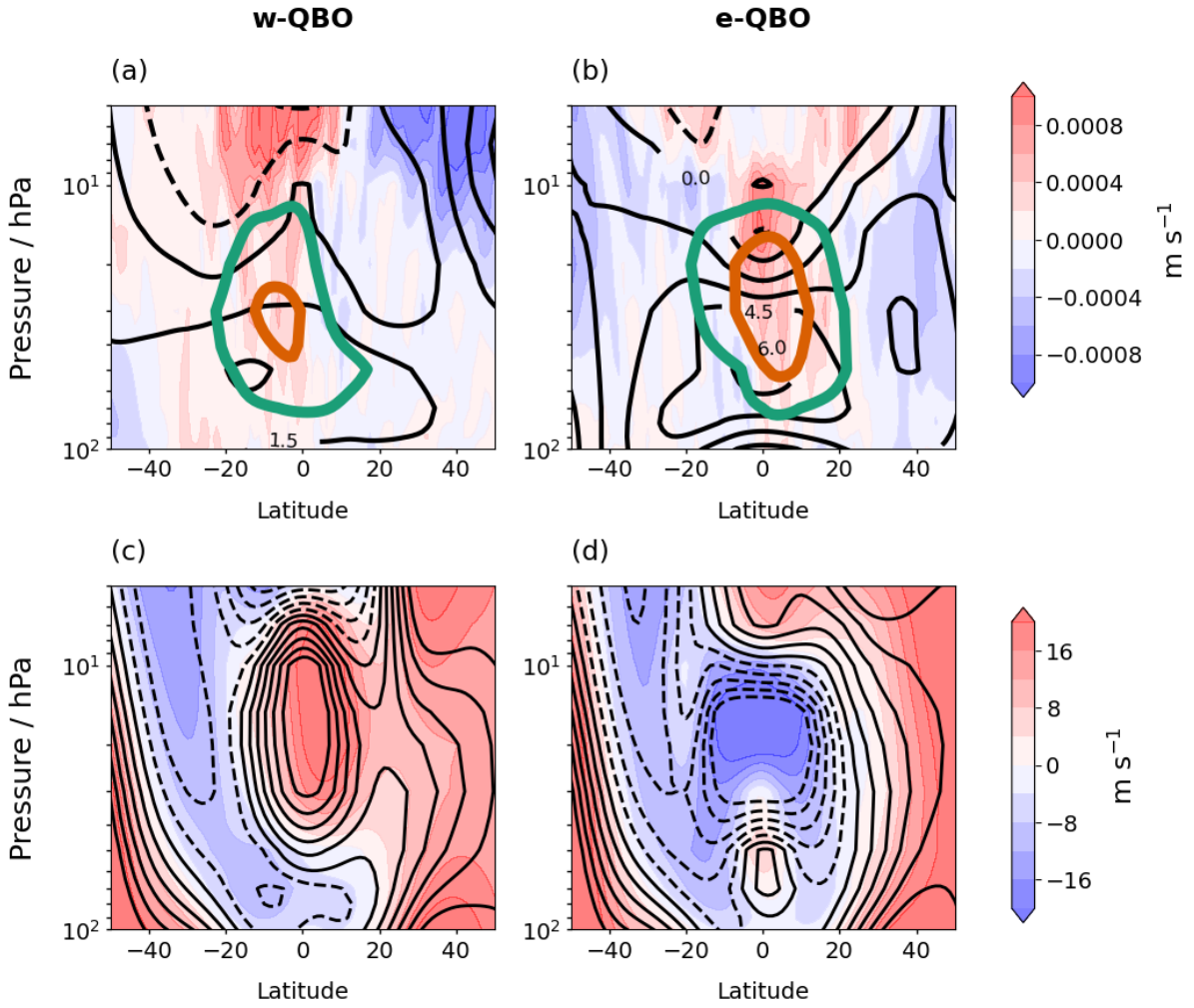

Figure S8: Five months after 15 Tg eruptions in July: (a), (b) shows the *w* anomalies (filled contours), positive temperature anomalies (black line contours) and sulfate mass mixing ratio anomalies (coloured line contours) with respect to the control ensemble mean. The sulfate mass mixing ratio contours are at interval of 5 x10^{-8}, 15 x10^{-8}, 50 x10^{-8} kg kg^{-1} and the temperature contours are in intervals of 1.5 K. (c), (d) The monthly mean zonal wind after the eruption (filled contours) compared to the control (black line contours). The filled contour intervals are the same as the line contours, with dashed lines representing negative zonal winds in the line contours. Panels (a) and (c) show results for the w-QBO, and panels (b) and (d), for the e-QBO.